

How the geometry makes the criticality in two - component spreading phenomena?

N I Lebovka^{†‡} § || and N V Vygornitskii[†]

† Institute of Biocolloid Chemistry NASU, 2, bulv. Vernadskogo, Kyiv, 252142, Ukraine

‡ Kyiv Mogyla Academy University, 2, vul. Scovorody, Kyiv, 252145, Ukraine

Abstract. We study numerically a two-component A-B spreading model (SMK model) for concave and convex radial growth of 2d-geometries. The seed is chosen to be an occupied circle line, and growth spreads inside the circle (concave geometry) or outside the circle (convex geometry). On the basis of generalised diffusion-annihilation equation for domain evolution, we derive the mean field relations describing quite well the results of numerical investigations. We conclude that the intrinsic universality of the SMK does not depend on the geometry and the dependence of criticality versus the curvature observed in numerical experiments is only an apparent effect. We discuss the dependence of the apparent critical exponent χ_a upon the spreading geometry and initial conditions.

PACS numbers: 05.40.+j, 05.70.Jk, 68.35.Rh, 81.15.-z, 82.20.Mj

Submitted to: *J. Phys. A: Math. Gen.*

1. Introduction

The nonequilibrium growth and spreading phenomena are common in nature. The examples may include such processes as irreversible adsorption or deposition on the surface, liquid invasion in porous media, forest fire, crystal growth, evolution of damages in mechanical or electrical systems, epidemic spreading, etc. Presently, the different varieties of such phenomena are extensively studied using the numerical models [1, 2, 3, 4, 5, 6]. The most simple models deal with the ideal species of the same size (or type) and the key attention is paid to investigation of interrelation between the growth mechanism, surface equilibration efficiency, details of interparticle interactions and pattern morphology.

But the ideal systems of monospecies quite rarely occur in nature and practically, certain variations of physical or structural properties are always present in such systems. The nonideal polydisperse or multicomponent systems are of a great scientific and practical interest [7, 8]. Recently, the various growth models with two species or phases competition [9, 10, 11, 12, 13, 14], and the multicomponent Potts growth model [15, 16] were investigated. The two-component growth model of Saito and Muller-Krumbhaar [9] generalises the Eden model [17] for the case of two different

§ To whom correspondence should be addressed.

|| E-mail: lebovka@roller.ukma.kiev.ua

species, A and B , competition (SMK-model). The authors [9] observe the criticality of the 2d-model for the case of equal growth rates of two components in a half-space planar geometry, i.e. for a case when the growth starts from the linear seed line. This criticality results from the rules of species attachment at the growing front, which exclude the nucleation of A species in a neighbourhood of domain consisting only of B species, and vice versa. The model reveals the competitive growth of separate domains and their coarsening. In the limit case of large time or height of the front, h , the power-law decay is found for N_{AB} domains,

$$N_{AB} \sim h^{-\chi}, \quad (1)$$

where N_{AB} is the number of domains and $\chi=2/3$ is the critical exponent for meandering interfaces [18]. Later on, Vandewalle and Ausloos [10] have come to a conclusion that the criticality of SMK model is not universal and depends on the assumed geometry of two-component propagation. They have shown that if the growth starts from the central sites of initial AB configuration, the value of the critical exponent χ may differ considerably from that observed for the half-space planar geometry ($\chi=2/3$). It should be noted that the geometry can effect the fractal dimension of DLA-like pattern in a closed cavity, as it was observed in [19]. Recently, Batchelor et al. [20] have shown, that for the usual 2d radial Eden model, the growing scaling exponent β governing the interface roughening exceeds considerably the value of $\beta=1/3$, which is typical for the stochastic growth on a planar substrate (in 1+1 dimensions), and only approaches this value in the asymptotic limit of the very large Eden cluster radius.

The present work studies kinetics of the two-component spreading on curved surfaces in assumption of SMK-model. The evolution of domains, their diffusion and annihilation takes place on a two-dimensional square lattice, and spreading is either confined inside the circle (concave geometry), or takes place outside the circle (convex geometry). For the infinitely large radius of the circle, $R \rightarrow \infty$, we revive the half-space or planar geometry [9], for other limit case of $R \rightarrow 0$ we consider the spreading in a free space [10]. So this modified model allows us to perform more precise control over the influence of geometry on criticality. Using the mean field diffusion-annihilation approach and simulations for SMK-model, we calculate the density profiles for wall boundaries between A and B domains as a function of distance from the seed wall h for seed circles of different radius, R . It will be shown that even in the case when criticality remains unchanged, the apparent value of the critical exponent of domain wall spatial distribution may vary and it depends on the geometry and initial distribution of A and B domains on the seed line.

The remainder of the paper is organised as follows: Section 2 presents a brief description of the model and simulation details. Section 3 is devoted to our results presentation and discussion. Section 3.1 contains theoretical discussions of the issue of universality for the competitive growth model with curved seed line. Here, we use the mean field approach for description of the domain walls coalescence. In the section 3.2 we present the results of a numerical simulation, performed using the SMK algorithm of [9] in order to test the theory exploited in section 3.1. Section 4 contains our conclusions.

2. Model and Simulation Details

We have used the simple two-component SMK growth model [9] with the equal growth rates of two components. The simulation takes place on the square lattice. In this model, same in Eden model, new particles attach the growing cluster only along its perimeter, however in the SMK model the probability of filling any empty site of perimeter either by A, or by B species, is in proportion to their concentration at the surface of propagation front. The growth starts from the circular seed line and develops as the growth front propagation for two different cases:

- Inside circular closed cavity. This is the case of concave geometry, or inside propagation (IP) case.
- Outside the circular closed cavity. This is the case of convex geometry, or outside propagation (OP) case.

The maximal size of studied systems was 2000×2000 grid points and inter-grid distance was set as $d = 1$. For each case, 100-500 samples were averaged.

The simulation was carried out for different ordered initial configurations, including case of a maximal density of domain boundaries with short correlation length $\lambda_d = 1$, where single A and B specie alternate, such as:

$$\dots | A | B | A | B | A | B | A | B | A | B | A | B | \dots, \quad (2)$$

and, also, in the case of lower densities of domain boundaries, with larger correlation length ($\lambda_d = 3$ for the case displayed), when there is an alternation of larger A and B species domains with equal length λ_d , such as

$$\dots | A | A | A | B | B | B | A | A | A | B | B | B | \dots. \quad (3)$$

If the initial number of domain boundaries is equal to N_{AB}^0 , then the initial linear density of the domains walls will be equal to $\rho_0 = N_{AB}^0/L$, where $L = 2\pi R$ is the length of the seed line. For the case displayed as the seed line (2) we have $\rho_0 = \rho_{max} \approx 1$ and

$$N_{AB}^0 = N_{max} \approx 2\pi R, \quad (4)$$

and for the more common case displayed as the seed line (3) we have $\rho_0 \approx 1/\lambda_d$ and $N_{AB}^0 \approx 2\pi R/\lambda_d$.

Figure 1 present the typical spreading pattern of IP case with the radius of closed cavity $R=1000$ (a) and the pattern of OP case with radius of circular exclusion $R=60$ (b). Here, the thin concentric lines are the time snapshots of the front evolution as at the moments of each next 300000 particles attachment. The thick lines show the AB inter-domain boundaries. In the OP case the simulation terminates when the maximal radius of growth front r_{max} reaches the boundaries of system ($r_{max}=1000$). The initial density of boundaries is chosen to be maximal, $\rho_0 = \rho_{max} \approx 1$ such as displayed in the seed line (2). Note, that for both IP and OP cases we observe the mostly quick decrease of the number of interdomain boundaries N_{AB} in initial periods of time, near the surface of circular seed line.

3. Results and Discussion

3.1. Mean Field Approach

The domain evolution can be described in the term of annihilations reaction of domain boundary. If we associate each domain boundary with fantom particle \hat{A} , then we can

consider the domain coarsening as diffusion-annihilation reaction of type $\hat{A} + \hat{A} \rightarrow \emptyset$ [9]. For the linear seed line the time evolution of the density $\rho = N_{AB}/L$ satisfies a mean-field rate equation

$$\frac{d\rho}{dh} = -a\rho^{1+1/\chi}, \quad (5)$$

giving $\rho \sim h^{-\chi}$, where h is the height of the front, or equivalently, is the time and a is the annihilation rate constant.

We have $\chi=1/2$ for the normal Brownian motion [21, 22, 23], and $\chi=2/3$ for a two-species Eden [18] or SMK [9] model.

Using the simulation for the planar geometry, we have estimated the annihilation rate constant as

$$a = 2.5 \pm 0.2, \quad (6)$$

where the data used in estimation were averaged over 100 different samples.

In a case of radial geometry the equation (5) should be modified. For this case we have additional source of ρ rate variations due to the shrinkage or dilation of the spreading front for the case of growth spreading inside the circle (concave geometry) or outside it (convex geometry), respectively. The domain density ρ at the distance $r = R \mp h$ from the centre of seed circle is equal to

$$\rho = \frac{N_{AB}}{2\pi(R \mp h)}, \quad (7)$$

where h is the distance from the seed circle, and, here and hereinafter, the upper sign (−) corresponds to the front spreading inside the seed circle (IP case, concave geometry) and the under sign (+) corresponds to the front spreading outside the seed circle (OP case, convex geometry). Taking the (7) into account we obtain instead (5) the following rate equation for the above-mentioned cases of radial spreading with $\rho(0)=\rho_0$ as initial condition:

$$\frac{d\rho}{dh} = -a\rho^{1+1/\chi} - \frac{\rho}{R \mp h}. \quad (8)$$

Introducing the new scaled variables $y=\rho R^\chi$, and $x=h/R$ we can rewrite (8) in scaled form

$$\frac{dy}{dx} = -ay^{1+1/\chi} - \frac{y}{1 \mp x}. \quad (9)$$

Equation (9) is a Bernoulli equation and substitution of $t=y^{-1/\chi}$ reduces it to the differential equation of the following type

$$\frac{dt}{dx} - \frac{t}{1 \mp x} = \frac{a}{\chi}. \quad (10)$$

The solution of (10) with initial condition of $t(0) = t_0 = \rho_0^{-1/\chi}/R$ has the following form

$$t(x) = t_0(1 \mp x)^{1/\chi} \left[\pm V(1 \mp x)^{1-1/\chi} + 1 \mp V \right], \quad (11)$$

where

$$V = a/(t_0(1 - \chi)) = aR\rho_0^{1/\chi}/(1 - \chi). \quad (12)$$

Taking into account the inverse substitution $y=t^{-\chi}$, we obtain the following final solution of differential equation (9)

$$y(x) = \frac{y_0}{(1 \mp x) [\pm V(1 \mp x)^{1-1/\chi} + 1 \mp V]^\chi}, \quad (13)$$

where $y_0 = \rho_0 R^\chi$.

For the IP case, when the spreading takes place inside the circle, the value $y(x)$ goes through the minimum at the point

$$x_{min}(V) = \begin{cases} 1 - \left(\frac{\chi}{1 - 1/V} \right)^{\frac{\chi}{\chi-1}} & \text{for } V \geq 1/(1-\chi), \\ 0 & \text{for } V < 1/(1-\chi). \end{cases} \quad (14)$$

For the case when $V \rightarrow \infty$, we have

$$x_{min} = \lim_{V \rightarrow \infty} x_{min}(V) = 1 - \chi^{\frac{\chi}{\chi-1}}, \quad (15)$$

and

$$y_{min} = \lim_{V \rightarrow \infty} y(x_{min}) = a^{-\chi} \chi^{\frac{-\chi^2}{1-\chi}}. \quad (16)$$

Figure 2 presents the y/y_{min} versus x dependencies obtained from (13), (16) for $\chi=2/3$ at different values of V for the case of growth spreading inside the circle (solid lines) and outside the circle (dashed lines). The slope value $-2/3$ accounts for the slope of lines in the limit $V \rightarrow \infty$ for the spreading both inside and outside the circle, and the slope value -1 accounts for the slope of the lines in the limit of $x \rightarrow \infty$ for the growth spreading outside the circle.

From (1), we can define the apparent value of the critical exponent χ_a as

$$\chi_a = -\frac{d \ln N_{AB}}{d \ln h}. \quad (17)$$

Figure 3 shows a plot of the apparent critical exponent χ_a versus scaled distance from the seed surface x for both concave (dash lines) and convex (solid lines) geometries. We see that for the propagation started from the curved seed line the value of the apparent exponent χ_a is not constant and strongly depends on x .

Not far from the seed surface, at $x \rightarrow 0$ and high initial density $\rho_0 = \rho_{max} \approx 1$ and in the limit $V \rightarrow \infty$, the intrinsic value $\chi_a = \chi = 2/3$ is observed. The observed χ_a values substantially decrease with initial density decrease. With increase of x , the value of χ_a always increases for the IP case. For the OP case, the χ_a goes through the maximum. We should stress that these are only apparent changes of critical exponents, estimated on the basis of (17), because all calculations were done for the universal system in assumption of constancy of intrinsic χ -value ($\chi = 2/3$).

3.2. Numerical Simulation

The dependencies of $y=\rho R^\chi$ upon $x=h/R$ obtained as results of numerical simulations are depicted in figure 4 for the IP case (a) and OP case (b). The different points correspond to the different radii of initial circular seed lines. All these data are obtained for the case of the maximal initial density of domain boundary $\rho_0 = \rho_{max} \approx 1$ with ordered configuration of A and B the species, as in the seed line (2). The continuum limit for this case corresponds to the situation when $R \gg 1$ and we can neglect the lattice discreteness. The solid lines in figure 4 obtained from (13) for

the case of $\chi=2/3$, $V \rightarrow \infty$ in the continuum limit. We see that in this limit the coincidence between the results of the mean field approximation and the computer simulation is rather good. It is important to note that in the limit of higher initial density of AB boundaries, all data obtained at different values of R in the scaled co-ordinates ρR^χ versus $x=h/R$ fall on the same curves for both IP and OP cases.

For the relatively small values of initial density ρ_0 , when we start propagation from configuration with limited number of domain boundary $N_{AB} \approx 10 - 100$, the simulation results can deviate substantially from predictions of the mean-field theory as it is shown on figure 5 for the IP case (a) and for the OP case (b). The reason of such deviation is unclear by far but we think that it simply reflects the limitations of the mean field approach, which follow from neglecting by the long range correlations between the AB domain boundaries.

4. Conclusions

We may conclude that the apparent critical exponent χ_a which is determined through treatment of the numerical experiments results for SMK model on the basis of (17), is not universal or constant value. For growth spreading in the case of nonplanar geometry the apparent critical exponent χ_a depends on the height of the AB front, initial numbers of AB domain and type of the spreading geometry. This conclusion remains true for SMK model even in the case when the model preserves its internal universality as defined by the classical critical exponent $\chi = 2/3$. The most good agreement between results of numerical simulation and of the mean field approximation is observed only at high initial number of boundaries N_{AB}^0 . At low initial number of boundaries N_{AB}^0 , the mean field approximation allows to reach only the qualitatively true description. In this case, the absence of quantitative description may be explained by the effect of long-range correlations, which result in the faults of the mean field description.

We believe, that results obtained in the present work coincide qualitatively quite well with data presented in [10]. The authors of this work have shown that for initial configuration consisting only from two species AB the number of boundaries is approximately conserved at the level of $N_{AB} \approx 2$ and in this case they obtained $\chi_a \approx 0$. Assuming for propagation under such conditions $N_{AB}^0 = 2$, $R \approx 1$, $\chi = 2/3$ and the value $a = 2.5 \pm 0.2$ (6) we have $V \approx 1$ as estimated from (12). As it follows from our data presented at figure 3, when the V values are so low, the χ_a value is small and practically equal to zero at high enough distances from the seed centre, which is in correlation with data obtained in [10]. We believe that such apparent alterations of criticality or scaling exponential functions may occur in other models of radial growth, as it was observed, e.g., in [20] for Eden model. The similar tasks are of interest for further investigations with the extended range of models, number of system components, space dimensionality, etc.

Acknowledgements

We are grateful to Marcel Ausloos, Barbara Drossel, Miroslav Kotrla, Sujata Tarafdar, and Nicolas Vandewalle for providing us with the preprints of their works and useful correspondence, and we thank Natalija Pivovarova for help with preparation of the manuscript. This work is partly supported by a grant QSU082112 from ISSEP.

References

- [1] Feder J 1988 *Fractals* (New York: Plenum)
- [2] Takayasu H 1990 *Fractals in the Physical Sciences* (Chichester: J. Wiley & Sons)
- [3] Avnir D (ed) 1992 *The Fractal Approach to Heterogeneous Chemistry: Surfaces, Colloids, Polymers* (Chichester: J. & Sons)
- [4] Vicsek T 1992 *Fractal Growth Phenomena* (Singapore: World Scientific)
- [5] Barabási A.-L. and Stanley H E 1995 *Fractal Concepts in Surface Growth* (Cambridge: Cambridge University Press)
- [6] Meakin P 1998 *Fractals, Scaling and Growth Far From Equilibrium* (Cambridge: Cambridge University Press)
- [7] Ren S Z, Tombácz E and Rice J A 1996 *Phys. Rev. E* **53** 2980
- [8] Tarafdar S and Shashwati R 1998 *Physica* B to be published
- [9] Saito Y and Muller-Krumbhaar H 1995 *Phys. Rev. Lett.* **74** 4325
- [10] Vandewalle N and Ausloos M, 1996 *Phys. Rev. E* **54** 3006
- [11] Drossel B and Kardar M 1997 *Phys. Rev. E* **55** 5026
- [12] Kotrla M and Predota M 1997 *Europhys. Lett.* **39** 251
- [13] Kotrla M, Predota M and Slanina F 1998 *Surf. Sci.* to be published
- [14] Batchelor M T, Henry B L and Watt S D 1998 *Physica* A to be published
- [15] Vandewalle N and Ausloos M, 1995 *Phys. Rev. E* **52** 3447
- [16] Vandewalle N, Ausloos M and Cloots R 1996 *J. Cryst. Growth* **169** 79
- [17] Eden M 1958 *Symposium on Information Theory in Biology* ed H P Yockey (New York: Pergamon) p 359
- [18] Derrida B and Dickman R 1991 *J. Phys. A: Math. Gen.* **24** L191
- [19] Lebovka N I, Vygornitskii N V and Mank V V 1997 *Colloid J.* **59** 310
- [20] Batchelor M T, Henry B L and Watt S D *Physica* A to be published
- [21] Smoluchowsky M V 1917 *Z. Phys. Chem.* **92** 129
- [22] Bramson M and Griffeath D 1980 *Ann. Probab.* **8** 183
- [23] Torney D C and McConnell H M 1983 *J. Phys. Chem.* **87** 1941

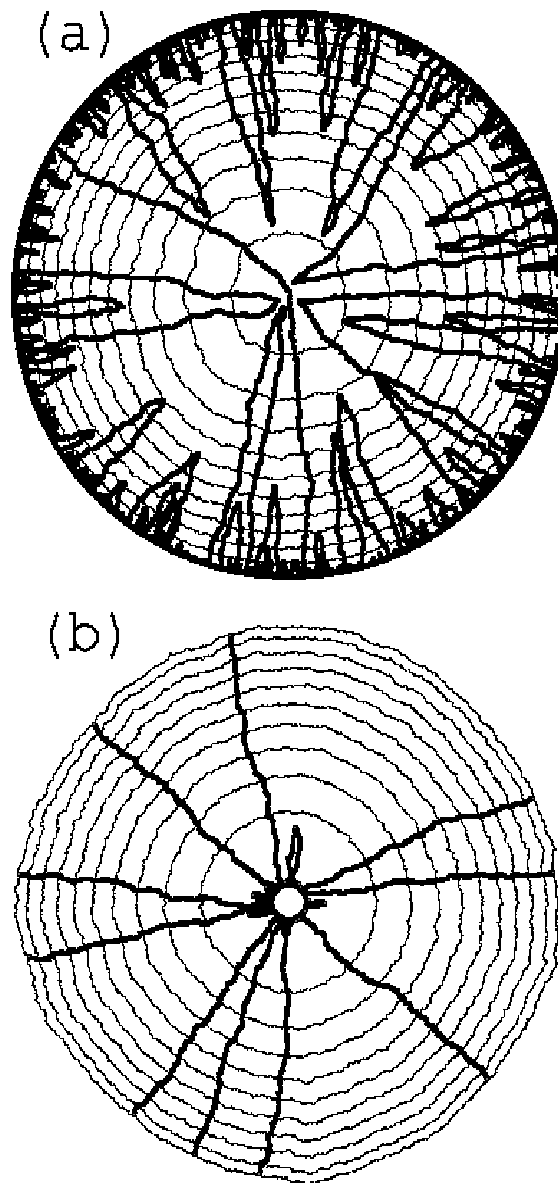


Figure 1. The typical growth spreading inside the circular cavity of radius $R=1000$ (a) and outside the circular exclusion of radius $R=60$ (b) for two-species SMK model. The thin concentrical lines are the time snapshots of fronts for each next group of 300000 particles attachment. The thick lines show the AB domain interfaces.

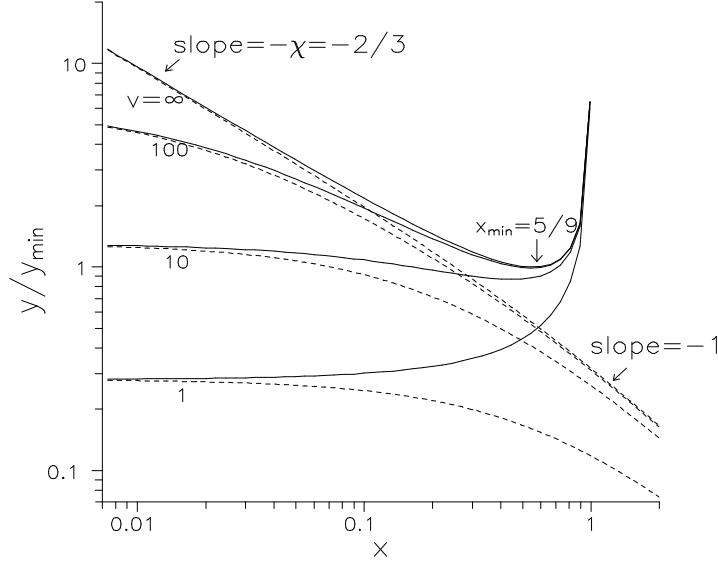


Figure 2. The mean field dependence of the scaled density y/y_{\min} ($y = \rho R^x$) versus scaled height of the front $x = h/R$ for the growth spreading inside the circular cavity (solid lines) and outside the circular exclusion (dashed lines) at different values of $V = aR\rho_0^{1/\chi}/(1 - \chi)$. The value of y_{\min} as defined by (16) corresponds to the minimum of $y(x)$ function in the point $x = x_{\min} = 5/9$ (for $\chi = 2/3$, see (15)) for growth spreading inside the circular cavity in the limit of $V \rightarrow \infty$.

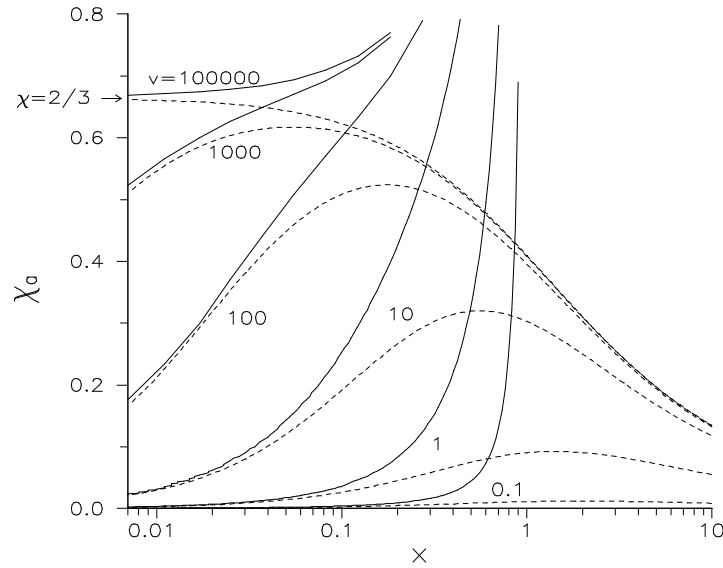


Figure 3. The effective critical exponent χ_α versus scaled distance from the seed surface $x = h/R$ for both concave (dash lines) and convex (solid lines) geometries at different values of $V = aR\rho_0^{1/\chi}/(1 - \chi)$. Arrow shows the classical value of $\chi = 2/3$ for the planar geometry.

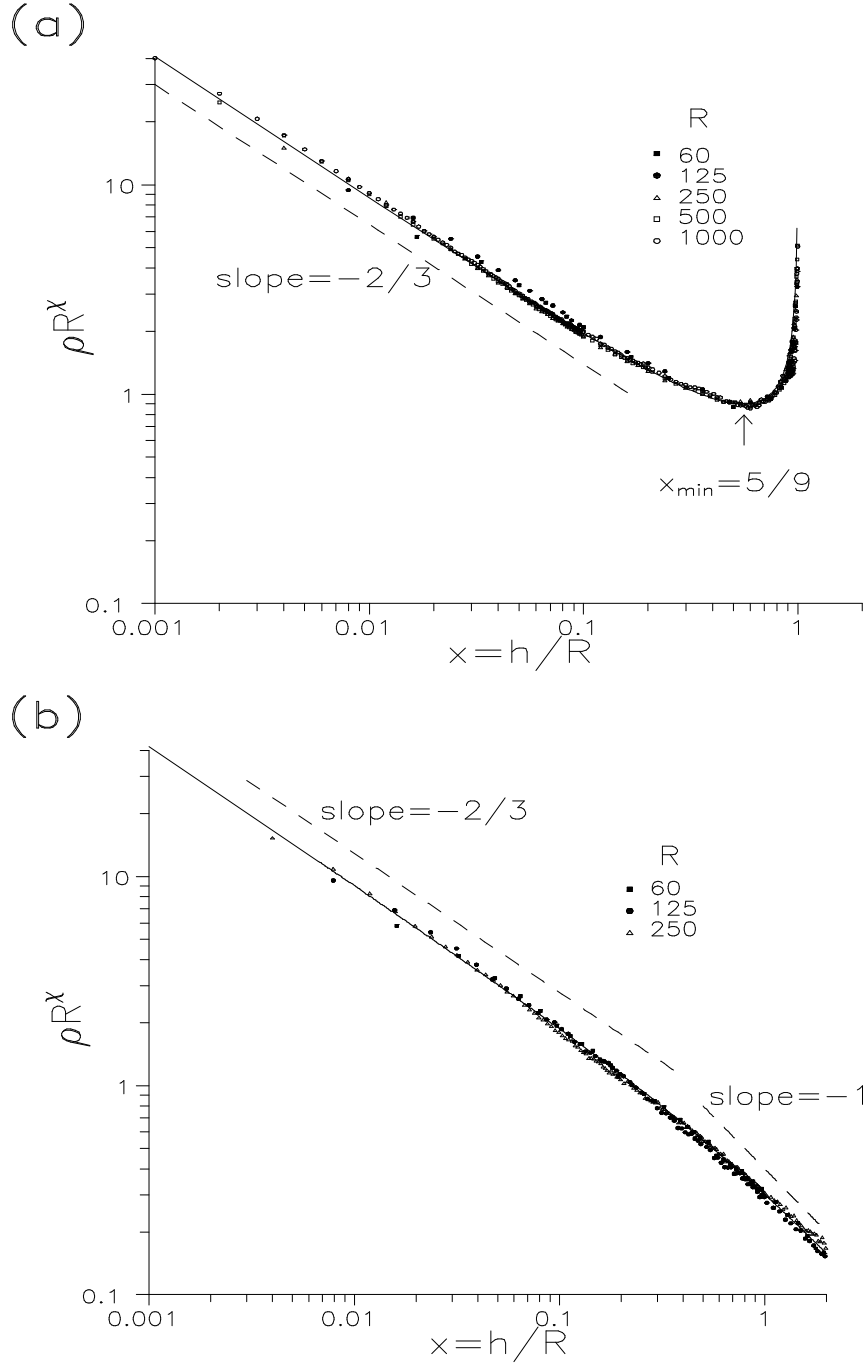


Figure 4. The scaled density $y = \rho R^\chi$ versus scaled height of the front $x = h/R$ for the growth spreading inside the circular cavity (a) and outside the circular exclusion (b). The different points are the simulation results for different cavity (a) or exclusion (b) radii, which are presented on the figures. All data are obtained for the limit case of $\rho_0 = \rho_{\max}$, for configuration shown by line (2). The solid lines are obtained from the mean field equation (13) where we used $a = 2.5 \pm 0.2$ (6) estimated by simulation for the case of planar geometry. Point of minimum $x = x_{\min} = 5/9 \approx 0.561$ is defined by the (15) for $\chi = 2/3$.

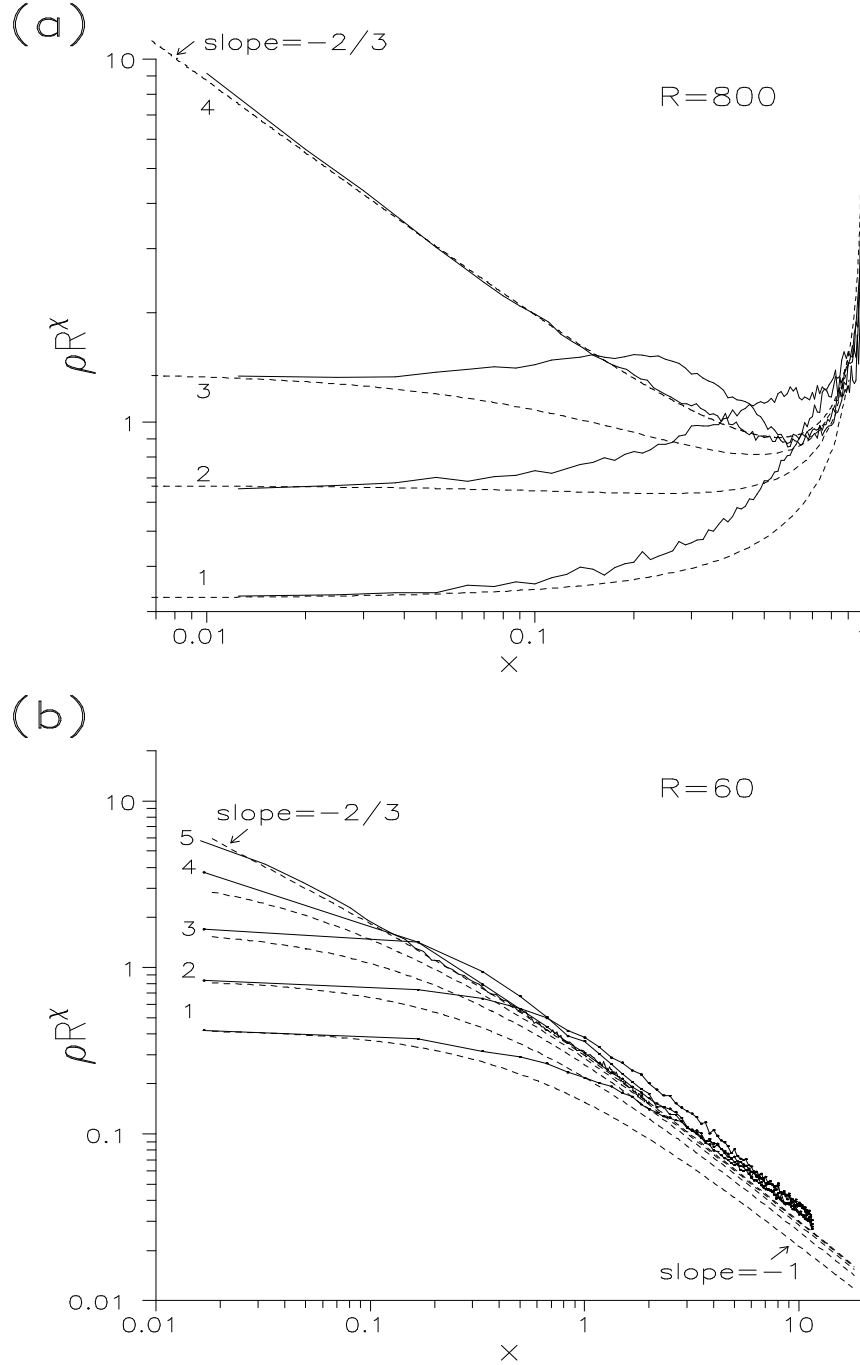


Figure 5. The scaled density $y = \rho R^x$ versus scaled height of the front $x = h/R$ for the growth spreading inside the circular cavity or radius $R = 800$ (a) and outside the circular exclusion or radius $R = 60$ (b). The solid irregular lines are the simulation results for different initial numbers of domain interfaces (a): $N_{AB}^0 = 20(1), 40(2), 80(3), N_{max}(4)$, and (b): $N_{AB}^0 = 10(1), 20(2), 40(3), 90(4), N_{max}(5)$. Dashed lines are obtained for the same numbers of domain interfaces through the mean field result (13) where we used $a = 2.5 \pm 0.2$ (6), estimated by simulation for the case of planar geometry.